BRAIN COMMUNICATIONS

Microstructural deficits of the thalamus in major depressive disorder

Yuxuan Zhang,[1,*] Yingli Zhang,[2,*] Hui Ai,[3] Nicholas T. Van Dam,[4] Long Qian,[5] Gangqiang Hou[6] and Pengfei Xu[1,7]

* These authors contributed equally to this work.

Macroscopic structural abnormalities in the thalamus and thalamic circuits have been implicated in the neuropathology of major depressive disorder. However, cytoarchitectonic properties underlying these macroscopic abnormalities remain unknown. Here, we examined systematic deficits of brain architecture in depression, from structural brain network organization to microstructural properties. A multi-modal neuroimaging approach including diffusion, anatomical and quantitative MRI was used to examine structural-related alternations in 56 patients with depression compared with 35 age- and sex-matched controls. The seed-based probabilistic tractography showed multiple alterations of structural connectivity within a set of subcortical areas and their connections to cortical regions in patients with depression. These subcortical regions included the putamen, thalamus and caudate, which are predominantly involved in the limbic-cortical-striatal-pallidal-thalamic network. Structural connectivity was disrupted within and between large-scale networks, including the subcortical network, default-mode network and salience network. Consistently, morphometric measurements, including cortical thickness and voxel-based morphometry, showed widespread volume reductions of these key regions in patients with depression. A conjunction analysis identified common structural alternations of the left orbitofrontal cortex, left putamen, bilateral thalamus and right amygdala across macro-modalities. Importantly, the microstructural properties, longitudinal relaxation time of the left thalamus was increased and inversely correlated with its grey matter volume in patients with depression. Together, this work to date provides the first macro–micro neuroimaging evidence for the structural abnormalities of the thalamus in patients with depression, shedding light on the neuropathological disruptions of the limbic-cortical-striatal-pallidal-thalamic circuit in major depressive disorder. These findings have implications in understanding the abnormal changes of brain structures across the development of depression.

1 Beijing Key Laboratory of Applied Experimental Psychology, National Demonstration Center for Experimental Psychology Education (BNU), Faculty of Psychology, Beijing Normal University, Beijing 100875, China
2 Department of Depressive Disorders, Shenzhen Kangning Hospital, Shenzhen Mental Health Center, Shenzhen 518020, China
3 Shenzhen Key Laboratory of Affective and Social Neuroscience, Magnetic Resonance Imaging Center, Center for Brain Disorders and Cognitive Sciences, Shenzhen University, Shenzhen 518052, China
4 Melbourne School of Psychological Sciences, The University of Melbourne, Melbourne 3010, Australia
5 MR Research, GE Healthcare, Beijing 100176, China
6 Department of Radiology, Shenzhen Kangning Hospital, Shenzhen Mental Health Center, Shenzhen 518020, China
7 Center for Neuroimaging, Shenzhen Institute of Neuroscience, Shenzhen 518107, China

Correspondence to: Pengfei Xu, PhD, Faculty of Psychology, Beijing Normal University, Beijing 100875, China.
E-mail: pxu@bnu.edu.cn

Correspondence may also be sent to: Gangqiang Hou, MD, Department of Radiology, Shenzhen Kangning Hospital, Shenzhen Mental Health Center, Shenzhen 518020, China. E-mail: nihaohgq@163.com

Keywords: depression; thalamus; structural connectivity; morphometry; quantitative MRI

Received March 28, 2022. Revised July 14, 2022. Accepted September 16, 2022. Advance access publication September 17, 2022

Abbreviations: AAL = automated anatomical labelling; DMN = default-mode network; DTI = diffusion tensor imaging; FA = fractional anisotropy; FDR = false discovery rate; GM = grey matter; GMV = grey matter volume; HC = healthy control; LCSPT = limbic-cortical-striatal-pallidal-thalamic; LN = limbic network; MDD = major depressive disorder; MNI = Montreal Neurological Institute; MTV = macromolecular tissue volume; NBS = network-based statistic; OFC = orbitofrontal cortex; PFC = prefrontal cortex; qMRI = quantitative MRI; ROI = region of interest; SBM = surface-based morphometry; SN = salience network; T1 = longitudinal relaxation time; VBM = voxel-based morphometry; WM = white matter; WMV = white matter volume

Graphical Abstract

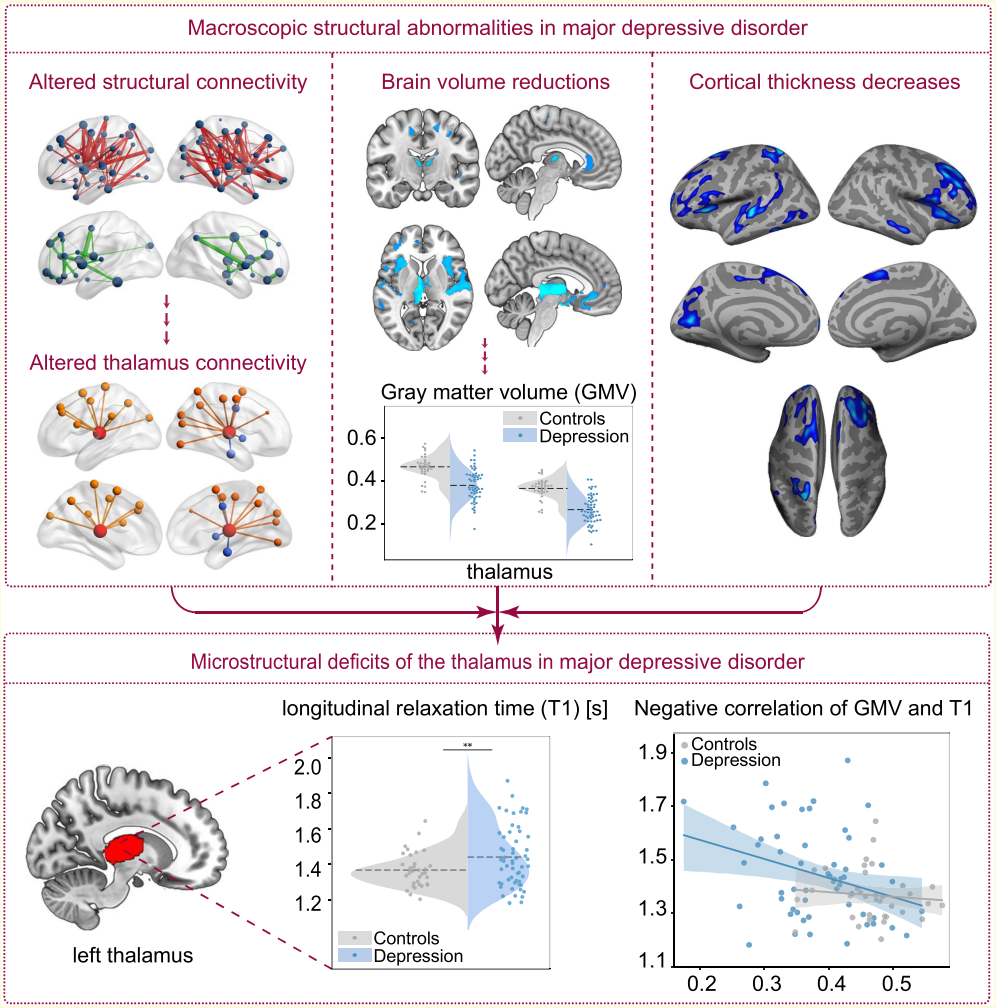

Introduction

Major depressive disorder (MDD) is a globally prevalent and burdensome psychiatric illness associated with abnormal changes in several cognitive domains, including attention, memory and emotion processing.[1] A large body of neuroimaging findings show structural deficits across multiple brain regions and widespread disruptions of connectivity between brain networks in MDD. These findings consistently converge on the limbic-cortical-striatal-pallidal-thalamic (LCSPT) circuit, which might underlie depressive pathology.[2–7] In support of this hypothesis, morphometric abnormalities have been observed across all parts of the LCSPT circuit in MDD, including grey matter volume (GMV) and/or white matter volume (WMV) reduction in the thalamus,[8,9] amygdala,[10] caudate,[11] putamen,[12] nucleus accumbens[13] and prefrontal cortex (PFC),[14] as well as cortical thickness decreases in the orbitofrontal cortex[15] (OFC). Complementary to the morphologic abnormalities, accumulating evidence has shown altered brain structural connectomes of key nodes within the LCSPT circuit in depression, involving decreased connectivity of white matter (WM) network and reduced grey matter (GM) structural covariance between the striatum, pallidum, thalamus and OFC.[16–20]

The thalamus is one of the key nodes within the LCSPT circuit. Anatomically interconnected with the PFC, striatum and amygdala, the thalamus serves as a hub in response to the relay and distribution of afferent signals.[2] Its reciprocal connections with cortical and subcortical regions enable the thalamus to facilitate exchanges of subcortical information with the cortex.[21] Neuroimaging findings have converged on thalamic involvement in macroscopic structural abnormalities in depression. Specifically, the thalamic volume reduction has been implicated in the pathophysiology of MDD and has been associated with severity of depressive symptoms.[22,23] Diffusion tensor imaging (DTI) studies have shown abnormal structural connectivity and reduced WM tracts within the thalamofrontal pathway in MDD.[17,18,24,25] By combining DTI with graph-theoretic approaches, disrupted topological organizations in key regions of the thalamic network have also been shown in MDD.[26,27] Collectively, these findings jointly converge upon structural abnormalities within the LCSPT circuit and its key nodes which may directly contribute to the neuropathology of MDD. Although macroscopic structural abnormalities in depression have been widely examined, quantitative alternations of cytoarchitectonic-related tissue properties underlying these macroscopic structural deficits in depression are not well understood.

By estimating brain macromolecular tissue volume (MTV) and longitudinal relaxation time (T1), the recently developed quantitative MRI (qMRI) technique can inform about macromolecular composition and organization.[28] Importantly, brain macromolecular compositions and contents are accompanied by a set of microstructural processes related to tissue properties. For example, axons with myelination can be encased by the protective sheath, which has a high macromolecular content.[29] These microstructural processes have been linked to macroscopic morphological changes of the brain.[30] Given the sensitivity and specificity of qMRI parameters, such as MTV and T1, to microstructural tissue properties,[28,29,31] we are able to quantify brain macromolecular composition *in vivo* and to make inferences about the underlying mechanism driving observed morphological findings. Specifically, MTV quantifies myelin volume on the basis that the brain macromolecules are principally cell membranes and proteins.[28] T1 depends on both density of macromolecules and the local microenvironment, thus can be used as a marker of microstructural changes during brain development, such as dendrites, oligodendrocytes and myelination.[32] Non-invasive brain tissue characterization using qMRI technique has significant implications for the identification of microstructural changes of specific regions and disease status monitoring in clinical practice.[28,32–37] For instance, studies of patients with depression have reported significantly changes in qMRI-related parameters, such as lower longitudinal relaxation rate, R1 (1/T1), and increased proton density, which have provided empirical evidence for microstructural changes of brain tissue composition and myelin in depression.[36,37] Therefore, the qMRI technique could be used to measure microscopic cytoarchitectonic-related properties underlying macroscopic structural alterations.

Here, we used a multi-modal neuroimaging approach comprising structural, diffusional and quantitative MRI to examine integrative structural abnormalities in patients with MDD, from macroscopic structural networks to the cytoarchitectonic-related microstructural level properties of the LCSPT circuit. We first explored abnormalities within- and across-network structural connectivity and the highly connected hub regions, as well as cortical thickness and subcortical volume across the whole brain. Next, we conducted a conjunction analysis to identify key regions that showed common structural alternations within the LCSPT circuit across multi-modal imaging data. Finally, we examined alternations in tissue properties as well as the relationship between tissue properties and macroscopic measurements of the identified key regions in MDD.

Materials and methods

Participants

In total, 56 MDD patients (aged 36 years, 41 females) and 35 age- and sex-matched healthy controls (HCs; aged 39 years, 22 females) were included in the present study. See Table 1 for details about demographic and clinical characteristics of all participants. For clinical details about the patients, see Supplementary Methods. All participants and/or the guardians of MDD patients had signed the informed consent before participating in the study. The study was approved by local ethics committee.

MRI data acquisition

All diffusion, anatomical and quantitative MRI data were collected from all participants ($n = 91$) using a 3 T GE Discovery MR750 scanner (GE Medical Systems) at Shenzhen Kangning Hospital with an eight-channel head coil (see Supplementary Methods for details of scanning parameters).

Table 1 Demographic and clinical characteristics of participants

	MDD ($n = 56$)	HC ($n = 35$)
Male sex, *n* (%)	15 (27)	13 (37)
Age, mean (SD), years	36.36 (15.96)	39.40 (14.77)
Educational level, mean (SD), years	12.82 (3.17)	14.94 (2.84)
HAMD score, mean (SD)	19.63 (7.61)	—
HAMA score, mean (SD)	16.23 (6.77)	—
Multiple depressive episodes, *n* (%)	22 (39)	—
Psychiatric comorbidities, *n* (%)	7 (13)	—
Current medications, *n* (%)	48 (86)	—
Duration exposed to medications, n (%)		
<3 months	24 (43)	—
≥3 months	24 (43)	—

HAMA, Hamilton anxiety rating scale; HAMD, Hamilton depression rating scale; HC, healthy control; MDD, major depressive disorder.

MRI data analysis

Diffusion MRI data analysis

The diffusion MRI data were first preprocessed followed by structural network construction and the network-based statistics (NBS) analysis[38] to evaluate the whole-brain structural connectivity in MDD patients (Fig. 1). An automated anatomical labelling (AAL) atlas[39] was used to parcellate the whole cerebral cortex into 90 regions/nodes (45 regions in each hemisphere, without the cerebellum; Supplementary Table 1) in native diffusion space, followed by probabilistic tractography between 90 AAL regions. This resulted in a connectivity matrix with inter-regional connection probability, representing a structural network for each participant. The NBS analysis was conducted to determine the difference of inter-regional structural connectivity between MDD and HC groups. Supra-threshold connections at a significant level of $P < 0.01$ with correction of family-wise error were reported. See Supplementary Methods for details.

For illustrating the connectivity patterns among large-scale brain networks in MDD patients, the identified increased and decreased structural connectivity were respectively categorized into an established seven-network parcellation of the human cerebral cortex with 100 parcels.[40] A total of seven networks were defined based on the parcellation scheme, including the visual network, sensorimotor network, dorsal attention network, salience network (SN), limbic network (LN), frontoparietal network and default-mode network (DMN). Given the importance of subcortical regions in our study, we included the subcortical regions as an additional network division. Each AAL region involved in disrupted structural connectivity was localized into the seven networks based on its Montreal Neurological Institute (MNI) centroid coordinates.

Anatomical MRI data analysis

Voxel-based morphometry (VBM) analysis using the VBM8 toolbox (http://dbm.neuro.uni-jena.de/vbm8/) as well as surface-based morphometry (SBM) analysis using Freesurfer[41,42] (http://surfer.nmr.mgh.harvard.edu) were performed to detect morphologic alternations in patients with MDD (Fig. 1; see Supplementary Methods).

Conjunction analysis

A conjunction analysis was conducted to identify regions that showed common alternations across all modalities, including structural connectivity, GMV/WMV and cortical thickness. Results from different analyses were integrated into AAL atlas based on the MNI coordinates of their peak voxel. The cortical regions were determined based on the consistent alternations across analyses of structural connectivity, VBM and SBM, while the subcortical regions were identified according to the analyses of structural connectivity and VBM. The identified regions, especially those play key roles within the LCSPT circuit, were included in subsequent qMRI analysis.

Quantitative MRI data analysis

The qMRI data were preprocessed by using the mrQ software package (https://github.com/mezera/mrQ) to produce the evaluation of MTV and quantitative T1 maps[28] (Fig. 1). To examine microstructural disruptions underlying the common alterations in structural connectivity and regional morphology, we conducted region of interest (ROI) analyses on the qMRI measurements of the regions identified in the conjunction analysis (for details, see Supplementary Methods).

We conducted Pearson correlation analyses to examine the relationships between microstructural properties (MTV/T1) and two other measurements, the GMV and fractional anisotropy (FA) within key regions identified by conjunction analysis. Correlation analysis was conducted to test the influence of anxiety on microstructural alternations (see Supplementary Methods).

Statistical analysis

Statistical analyses were performed using IBM SPSS (version 20). The χ^2 test and t-test were conducted to compare potential between-group differences in gender, age and education, with a statistical significance of $P < 0.05$. For the volumes of subcortical regions, a general linear model was conducted controlling for overall brain volume and participants' demographic variables (age, sex and education years) with a statistical significance of $P < 0.05$ after false discovery rate (FDR) correction. For ROI analysis of qMRI data, a two-sample t-test was conducted with participants' age and gender as covariates to test group difference in MTV and T1 within each ROI. Significance was set at $P < 0.05$, FDR corrected.

Data availability

The datasets reported in the current study are available upon request from the corresponding author. The data analysis scripts and codes generated and used in this work are available through the OSF (https://osf.io/6vpks/).

Results

Demographic and clinical characteristics

There were no significant differences in age nor gender between MDD patients and HCs (age: $t_{(89)} = -0.910$, $P = 0.365$; gender: $\chi^2_{(1)} = 1.085$, $P = 0.353$), but a significant group difference in years of education ($t_{(89)} = -3.228$, $P = 0.002$). We then repeated the MRI data analyses with and without the demographic data as covariates to test whether our results of MRI data analyses were affected by the demographic data. The results were robust after controlling for demographic variables (for details, see Supplementary Results).

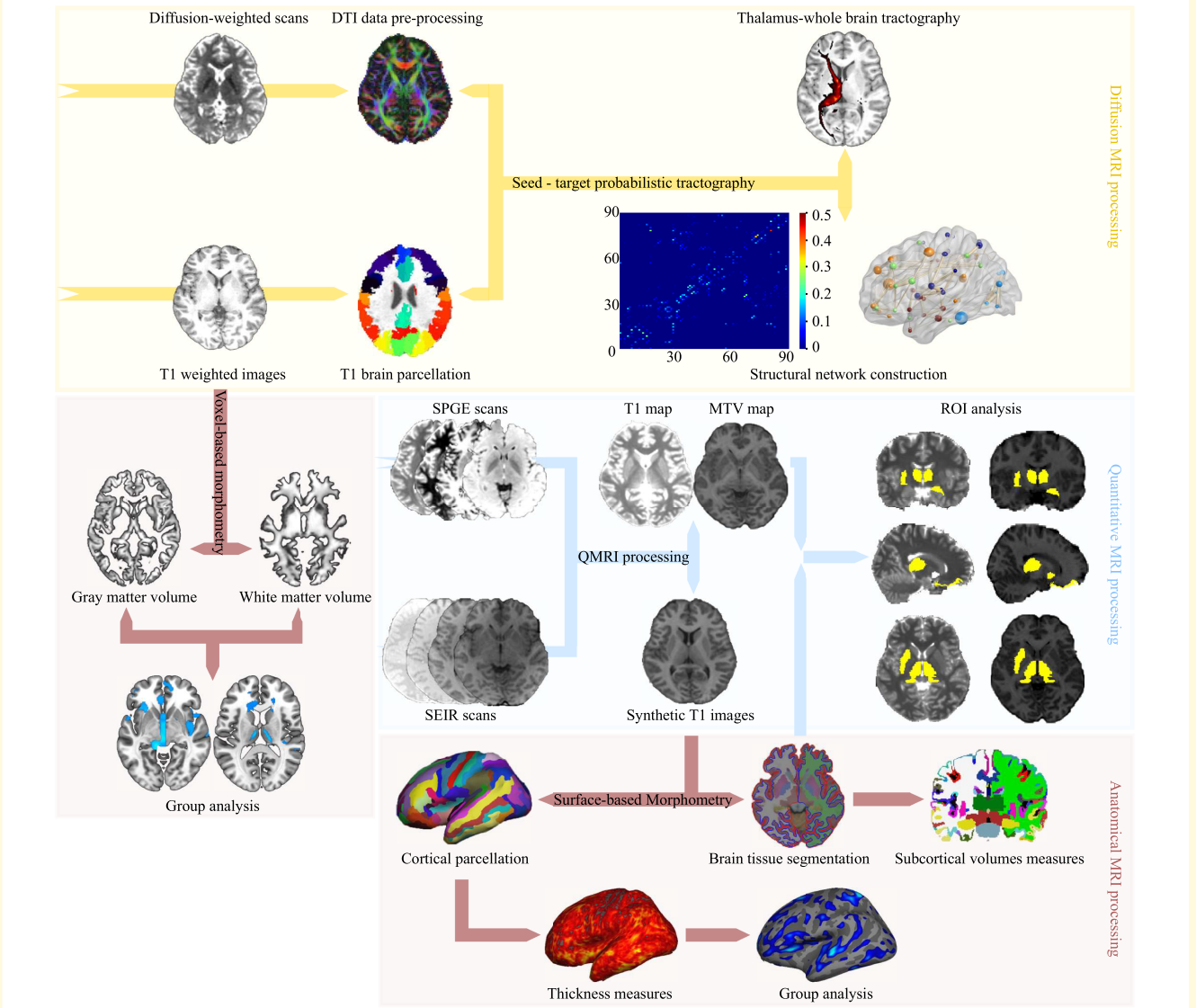

Figure 1 An overview of the MRI data analysis workflow. In diffusion MRI processing stream, the DTI model was constructed from the individual diffusion-weighted image. The T1-weighted brain images were parcellated into 90 cortical and subcortical regions according to the AAL atlas. Using 'seed-target' probabilistic tractography, the thalamus-specific connectivity and the whole-brain structural network were constructed. In quantitative MRI processing stream, the MTV and T1 maps with synthetic T1 images were generated and used for ROI analysis. In anatomical MRI processing stream, the synthetic T1 images were processed for the qMRI ROI analysis and SBM analysis. Additionally, individual T1-weighted images were processed for VBM analysis. DTI, diffusion tensor imaging; SPGE, spoiled gradient echo; SEIR, spin echo inversion recovery; MTV, macromolecular tissue volume; ROI, region of interest; SBM, surface-based morphometry; VBM, voxel-based morphometry.

Alternations of whole-brain structural connectivity in MDD

The NBS analysis showed two networks with disrupted structural connectivity in patients with MDD (Fig. 2). Specifically, one network comprised of 215 edges that connected to 76 nodes, showing significant increased structural connectivity in MDD (Fig. 2A, MDD > HC). The other network consisted of 44 edges linking to 38 nodes, showing significant decreased structural connectivity in MDD (Fig. 2B, MDD < HC).

At the large-scale networks level, we found that the most increased/decreased structural connections were those within the subcortical network, as well as those between the subcortical regions and cortical networks, including the DMN, SN and LN (Fig. 2C and D). Specifically, the increased structural connections within the subcortical network were observed between the HIP.R and left putamen (PUT.L; $t = 3.56$), the left thalamus (THA.L) and the right putamen (PUT.R; $t = 3.39$), the HIP.R and the left amygdala (AMYG.L; $t = 3.32$), the PUT.L and the right pallidum (PAL.R; $t = 3.31$), the AMYG.L and the left caudate

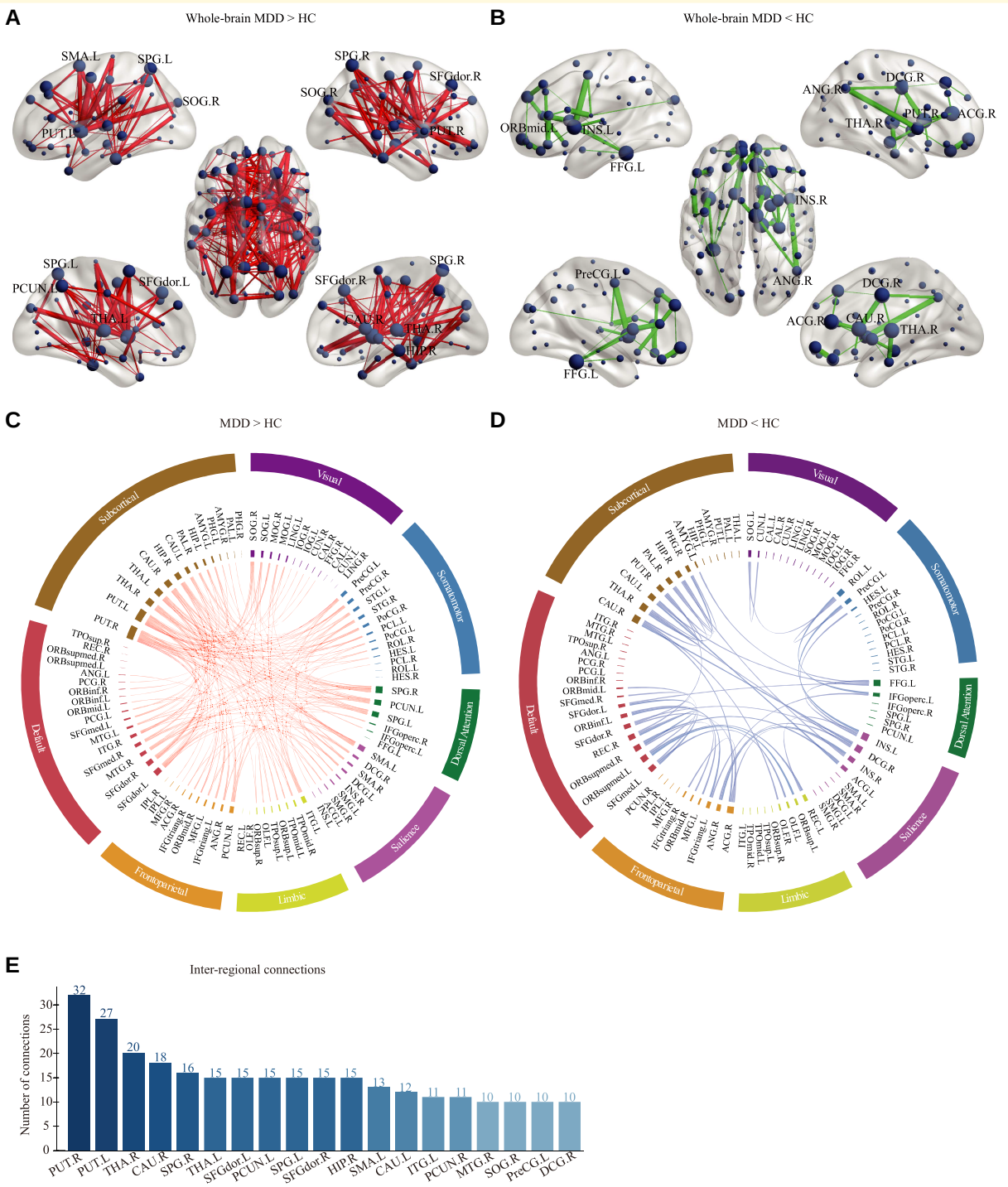

Figure 2 Altered structural connectivity in MDD patients. (**A**) Increased and (**B**) decreased connectivity identified by the NBS analysis in MDD patients relative to HCs. The node size indicates the number of edges connecting to the given node. Nodes with ≥10 increased connections or ≥4 decreased connections are labelled. The edge width represents the *t* value of connectivity between nodes. The circle plots depict (**C**) increased and (**D**) decreased connectivity patterns within and between seven networks and subcortical network. The AAL regions are represented by the inner segments of circle plots and are circularly arranged according to their number of connections. The angular size of each inner segment is proportional to the total connections of the given region. Networks are labelled on the outer segments. Regions within the same networks are shown in the same colour. The *t* values of connections are represented by ribbons between the inner segments. (**E**) The hub regions with ≥10 inter-regional connections (both increased and decreased) in the whole-brain structural connectivity are sorted in descending order. DA, dorsal attention; HCs, healthy controls; MDD, major depressive disorder. For abbreviations and indices of AAL regions, see Supplementary Table 1.

(CAU.L; $t = 3.26$), the left hippocampus and the PUT.R ($t = 3.31$) and the HIP.R and the THA.L ($t = 2.91$). On the other hand, the decreased connectivity within the subcortical network included in the connections of the HIP.R with the PUT.R ($t = 3.23$) and PAL.R ($t = 2.94$), and the connections of the THA.R with the right parahippocampal gyrus ($t = 3.64$) and CAU.L ($t = 3.45$). With regard to the between-network connectivity, the increased between-network connectivity was expressed largely between the subcortical network and nodes of the DMN, specifically the THA.L and the left dorsolateral superior frontal gyrus (SFGdor.L; $t = 3.24$), the THA.L and the right dorsolateral superior frontal gyrus (SFGdor.R; $t = 2.67$), the THA.R and the SFGdor.L ($t = 2.70$), the CAU.R and the SFGdor.R ($t = 3.38$) and right medial superior frontal gyrus ($t = 3.31$), the PUT.R and the SFGdor.L ($t = 3.88$), SFGdor.R ($t = 3.79$) and right inferior orbitofrontal gyrus ($t = 3.45$) and between the HIP.R and the SFGdor.R ($t = 2.74$). The decreased between-network connectivity was mainly between the left superior medial orbitofrontal gyrus of the DMN and the left superior orbitofrontal gyrus of the LN ($t = 4.18$), and between the DCG.R of the SN and the CAU.R ($t = 3.78$) and THA.R ($t = 2.88$) of the subcortical network.

Grey/white matter volume alternations in MDD

Significant group differences were observed in both GMV and WMV (Fig. 3 and Table 2). The reduced GMV/WMV in MDD was not significantly influenced by the covariates (see Supplementary Results). There was no region showing larger GMV or WMV in MDD patients than in HCs.

Cortical thickness and subcortical volume alternations in MDD

We found 14 clusters where cortical thickness was significantly lower in MDD patients relative to HCs (Fig. 4 and Table 3). No significant increases in cortical thickness were detected in the MDD group. None of the subcortical volumes showed significant group differences with FDR correction.

Cross-modality structural alternations in MDD

The conjunction analysis identified five regions with common cross-modal structural alternations. Specifically, there

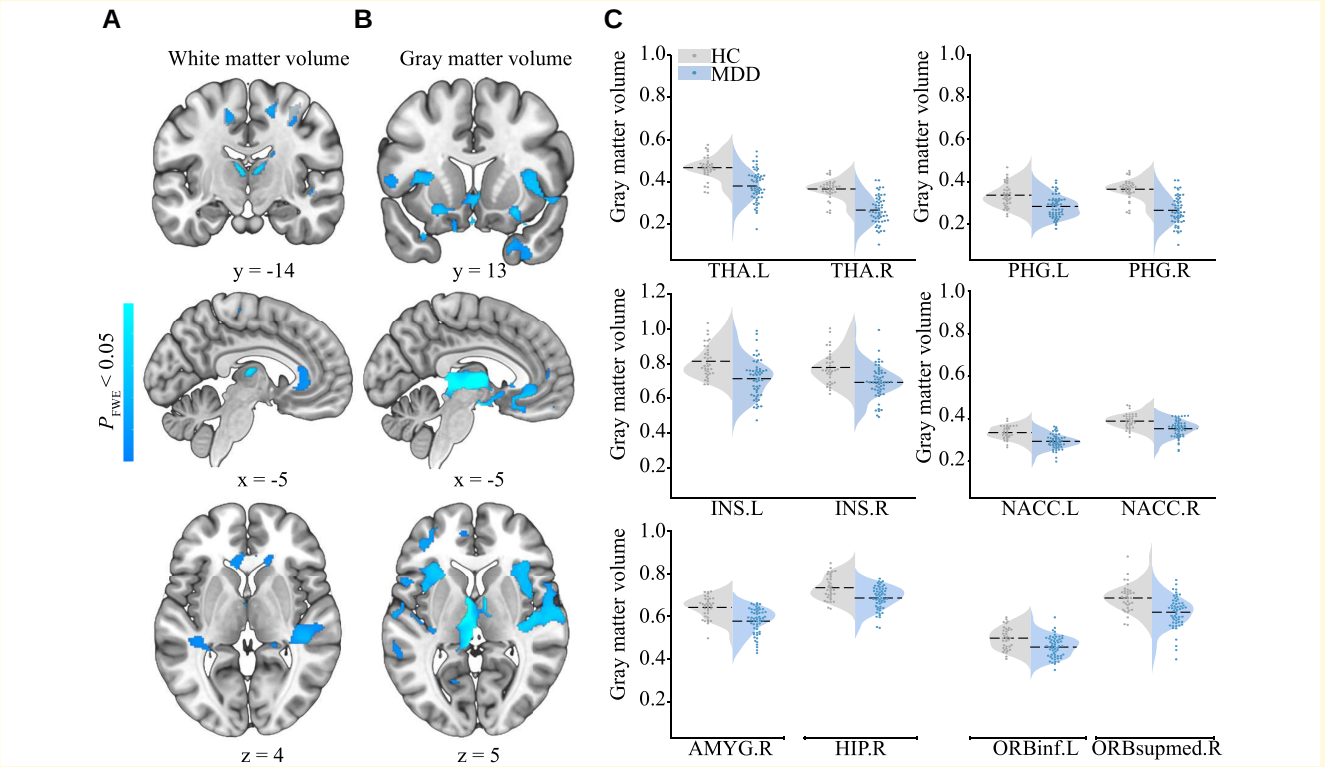

Figure 3 Between-group differences in white matter volume and grey matter volume. (**A**) The white matter volume (WMV) and (**B**) grey matter volume (GMV) reductions in MDD patients compared with HCs. The colour bar indicates *P*-value. Representative coronal, sagittal and axial slices of the supra-threshold clusters were overlaid on a MNI152 template. (**C**) The violin plots depict between-group differences of the GMV values within 12 key regions, where the width indicates subject density, the dashed line indicates average grey matter volume and the scatters indicate subject distribution for each group. Because the raw statistic map was transformed into TFCE values, only for the purpose of display, the GMV values of these regions were derived from the voxel-level statistic map obtained by using two-sample *t*-test with the threshold of $P < 0.001$ (uncorrected). HC, healthy control; MDD, major depressive disorder; NACC, nucleus accumbens. For abbreviations of AAL regions, see Supplementary Table 1.

were one cortical, the left middle orbitofrontal gyrus, and four subcortical regions, the left putamen, right amygdala and bilateral thalamus, involved across structural connectivity and morphologic features (Supplementary Table 2).

Microstructural alternations of the thalamus in MDD

MTV/T1 alternations. We found the averaged T1 values were significantly higher in MDD patients than in HCs in the left thalamus (THA.L; $t_{(89)} = 2.687$, $P = 0.009$; Fig. 5B). This result was not significantly correlated with levels of education ($r = -0.193$, $P = 0.067$) or anxiety ($r = -0.259$, $P = 0.127$). No significant between-group difference in qMRI measures was observed in other ROIs after FDR correction.

Relationships of microstructural changes with macroscopic alternations. The correlation analysis of qMRI measurements showed that T1s were inversely correlated with the GMV values in the THA.L ($r = -0.307$, $P = 0.023$; Fig. 5C) specifically in MDD but not in HCs. There was no significant correlation observed between T1s and FA values in the THA.L in MDD group ($r = -0.109$, $P = 0.423$).

Discussion

To our knowledge, this is the first study combining macro–micro neuroimaging techniques to characterize structural abnormalities of the neural pathway that underlies the neuropathology of MDD. Three main findings are revealed in the present study. First, subcortical regions involved in neural circuits of MDD exhibit disrupted within- and between-network connectivity. Second, hub regions that are highly interconnected in structural networks consistently show morphological abnormalities. Third, the thalamus of the LCSPT circuit exhibits both across modal macrostructural alternations and cytoarchitectonic-related abnormalities in MDD. These findings elucidate the primary role of the thalamus in macro-to-micro structural abnormalities of depression.

Disrupted structural brain networks in MDD

We found that patients with MDD were characterized by abnormal structural connectivity within subcortical network and between the subcortical network and DMN/SN. Consistent with previous findings,[24,26,27] these results suggest the centric roles of the subcortical areas in disrupted brain connectivity of MDD. Importantly, these subcortical structures, including the bilateral thalamus, bilateral putamen and right caudate, are highly connected, responsible for the normal regulation of mood and involved in a variety of neural circuits of MDD.[2,3] Evidence from neuroimaging and neuropathological studies suggests that abnormalities within and between these structures potentially account for disturbances in emotional behaviour and other aspects of depressive syndromes.[43,44] For example, disrupted WM connectivity within the frontal-subcortical networks,[24] as well as decreased WM tracts in the frontothalamic loops have been found in depressed patients.[25] These hub regions form the LCSPT circuit, which is known for its central involvement in mood disorders like depression.[2–4]

Of this circuit, the thalamus is critical for cognitive and emotional processes through its higher order relay. Among the

Table 2 Clusters showed significant grey/white matter volume differences between MDD patients and HCs

Anatomical region[a]	Side	MNI coordinates[b] x	y	z	Cluster size	*P*-value
GMV						
THA	L	−8	−6	4	1112	<0.001
AMYG	R	21	0	−15	353	0.001
HIP	R	18	−9	−15	265	0.001
PHG	L	−20	−26	−18	516	0.002
PHG	R	14	0	−18	407	0.002
THA	R	10	−9	7	328	0.005
STG	R	65	−20	12	2480	0.005
INS	L	−32	24	0	1345	0.005
HES	R	39	−24	9	528	0.005
ORBinf	L	−21	18	−14	583	0.006
PUT	L	−24	17	6	187	0.006
REC	R	2	51	−18	551	0.007
OLF	L	−20	6	−12	391	0.007
SMG	R	56	−33	27	672	0.008
INS	R	39	11	2	2259	0.009
REC	L	0	49	−18	925	0.009
ORBsupmed	R	9	51	−12	768	0.009
ACG	L	−4	35	−9	423	0.009
MTG	R	66	−22	−3	160	0.010
STG	L	−60	−17	9	1731	0.017
MFG	L	−33	50	1	280	0.017
HES	L	−51	−16	10	299	0.018
TPOmid	R	21	12	−36	522	0.019
ORBmid	L	−39	45	0	193	0.019
FFG	R	28	5	−41	687	0.021
SFGdor	L	−16	50	34	808	0.027
MTG	L	−63	−33	2	382	0.035
WMV						
THA	R	10	−22	9	613	0.004
THA	L	−6	−15	10	431	0.006
PreCG	R	32	−19	57	1192	0.010
PreCG	L	−28	−22	55	625	0.015
PoCG	L	−26	−40	48	608	0.017
SMA	R	9	−27	58	446	0.017
PCL	R	6	−30	61	330	0.018
PCUN	L	−15	−42	60	244	0.018
DCG	L	−14	−16	45	214	0.021
CAU	R	16	−18	21	397	0.022
IFGoperc	R	36	8	30	128	0.029
SFGdor	R	15	11	54	302	0.030
PoCG	R	30	−27	60	217	0.031
ACG	L	−3	35	−2	180	0.031
STG	R	56	−24	1	862	0.034

GMV, grey matter volume; HC, healthy control; L, left; MDD, major depressive disorder; R, right; WMV, white matter volume.
[a]For full names of these abbreviations from AAL atlas, see Supplementary Table 1.
[b]The MNI coordinates of the voxel with maximum statistical significance for identified clusters. Each cluster was represented by a coordinate of the peak voxel in this cluster.

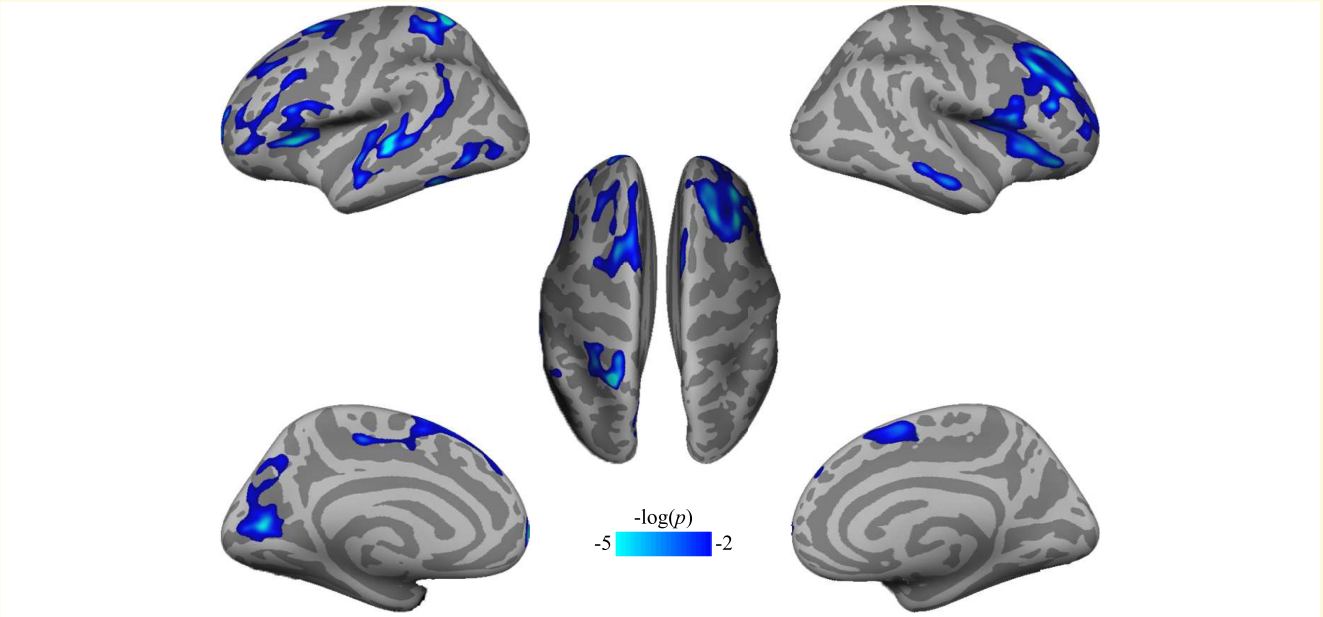

Figure 4 Cortical thickness decreases in MDD patients compared with HCs. Significant differences in cortex thickness were mapped onto the bilateral inflated cortical surfaces at the lateral and medial views. The colour bar represents *P*-value. L, left hemisphere; R, right hemisphere.

Table 3 Surface-based cluster summary of significant differences in cortex thickness between MDD patients and HCs

Anatomical location[a]	Side	Size (mm^2)	MNI coordinates[b]			CWP
			x	y	z	
MFG	R	3790.43	37.1	27.3	39.9	0.0002
MTG	L	2277.56	−62.2	−21.5	1.8	0.0002
ORBinf	R	2141.24	43.5	33.5	−13.3	0.0002
SFGdor	L	1739.25	−19.5	10.3	56.0	0.0002
CAL	L	1696.76	−15.4	−77.3	10.9	0.0002
SPG	L	1170.05	−25.5	−54.8	63.6	0.0002
INS	L	1163.41	−31.9	26.5	9.0	0.0002
ORBmid	L	1138.21	−38.4	44.7	−3.8	0.0002
SFGmed	L	667.90	−11.7	63.0	2.5	0.0024
ITG	L	529.68	−49.8	−62.8	−5.9	0.014
ITG	L	502.62	−50.3	−48.8	−17.2	0.019
MFG	L	488.18	−25.7	28.4	33.5	0.023
SMA	R	481.17	7.4	4.5	59.7	0.030
MTG	R	471.28	60.0	−15.6	−16.8	0.034

CWP, cluster-wise *P*-value; HC, healthy control; L, left; MDD, major depressive disorder; R, right.
[a]For full names of these abbreviations from AAL atlas, see Supplementary Table 1.
[b]Coordinates of the peak vertex for this cluster.

higher order thalamic relay nuclei, the mediodorsal thalamic nucleus has reciprocal connections with the PFC, relaying substantial subcortical projections from the amygdala and parahippocampal cortex to the orbital and medial PFC.[2,4] Given its broad connections with cortical and subcortical structures, growing evidence suggests mapping thalamic connectivity can help to characterize distributed circuits abnormalities in neuropsychiatric disorders.[45] In this context, our findings show increased connections of the thalamus with the PFC, bilateral putamen, caudate and pallidum in depression, which are key components of the LCSPT circuit. These findings provide multi-modal neuroimaging evidence for the neuropathology of MDD, where the thalamus plays a central role, connecting from prefrontal top–down control regions to the amygdala and putamen that responsible for the bottom–up processing of emotional signals.

At the network level, a lot of evidence has shown abnormalities in functional connectivity within the DMN and SN in depression.[46,47] By synthesizing these findings, a triple network model has been proposed to particularly emphasizes the roles of the DMN and SN in abnormal patterns of functional connectivity in the depressed brain.[48] Our findings revealed disrupted structural connectivity within the DMN and SN in MDD patients. Specifically, the precuneus of DMN and the insula of SN were involved in most of the abnormal connections with nodes of subcortical network, e.g. the putamen, thalamus, caudate and hippocampus. We suggest that these key nodes represent structural hubs particularly sensitive to network-level disruptions in MDD. Notably, the structural hubs we identified are also known to be functionally altered in depression based on previous evidence of functional connectivity.[49] Taken together, these findings support the triple network model in depression by providing evidence of both structural and functional connectivity.

Abnormal morphometry alternations in MDD

The hub regions altered in network connectivity also showed abnormal morphologic alterations, with specific volumetric

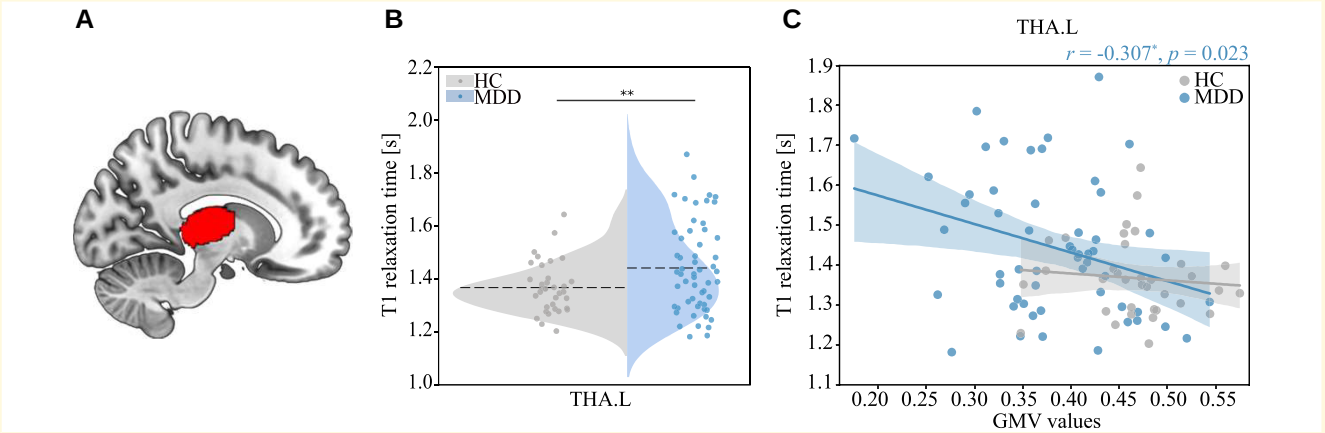

Figure 5 Group differences in T1 values and the correlation with grey matter volume. (**A**) The volumetric mask of the left thalamus was mapped on a MNI152 template for visualization. (**B**) The violin plot shows between-group differences in T1s in the left thalamus using two-sample *t*-test ($t_{(89)} = 2.687$, $P = 0.009$). (**C**) Correlation between grey matter volume and T1 values in the left thalamus in MDD group. The correlation coefficient (*r*) and *P*-value in MDD group were shown on the upper right of the plot. Note that the left thalamus was segmented based on Destrieux Atlas in individual space. GMV, grey matter volume; HC, healthy control; MDD, major depressive disorder; THA.L, the left thalamus.

losses and thickness decreases. Volume losses in subcortical structures of the LCSPT circuit have been associated with the pathology of MDD,[44] and have been proposed as potential markers of MDD.[50] For example, the reduced thalamus volume has been observed in the first-episode, untreated MDD patients,[9] which was thought to help account for its maladaptive bottom–up processing of negative stimuli in MDD, and therefore is considered to be a potential marker of MDD.[23] A recent meta-analysis has shown the corpus striatum, which comprises the caudate and putamen, was smaller in MDD.[10] Especially, volume reduction of the caudate has been more extensively studied in depression and has shown to be associated with suicidality.[51] Our findings showed both the GMV and WMV of the bilateral thalamus and GMV of the left putamen were reduced in MDD patients, which confirm the morphologic abnormalities of the thalamus and striatum in MDD. Crucially, our results showed consistently morphologic abnormalities and disrupted structural connectivity of the bilateral thalamus, right hippocampus and left putamen, suggesting the dysconnectivity within the LCSPT circuit in MDD. Besides, we also observed disrupted structural connectivity and decreased GMV and thickness of the left insula, one of key regions in the detection of 'salient', suggesting structural deficits of the insula also contribute to the neuropathology of MDD.

Numerous studies have shown widespread GMV/WMV reductions in MDD, especially the hippocampus, which is one of the most predominant regions that consistently showing volume reduction,[10,52] suggesting hippocampal abnormality is a contributor to the pathogenesis of depression. Previous studies have also shown volume reductions as well as cortical thinning of the PFC and OFC in MDD.[14,53,54] Consistently, we found reduced GMV of the right hippocampus, reduced PFC and OFC volume and decreased OFC thickness in bilateral hemispheres, suggesting critical roles of these brain regions in the neuropathology of depression. Taken together, our findings provide multimodal neuroimaging evidence for the structural abnormalities of the LCSPT circuit in MDD. These findings are informative with regard to the neurobiological mechanisms that underlying cognitive and affective impairments in MDD.

Abnormal microstructural alternations of the thalamus in MDD

Our study has revealed for the first time that cytoarchitectonic-related properties of the thalamus were altered in the depressive brain, while the thalamus was also involved in macroscopic structural abnormalities including disrupted structural connectivity and volume reductions in MDD patients. As aforementioned, we observed that a set of 'key regions' were involved in common structural abnormalities in MDD across multimodalities. These key regions formed the LCSPT circuit, which is associated with depressive symptoms,[3,4,55,56] as well as emotional and cognitive deficits in MDD.[5,57,58] For example, the structural abnormalities of the thalamus such as volume loss are thought to be associated with its dysfunction in MDD.[23]

Given T1 decrease has been associated with the developmental change of brain tissue,[32] larger T1 of the left thalamus in our study reflects abnormal development of the thalamus in MDD patients. Because T1 is sensitive to both MTV and tissue composition,[32] larger T1 could be driven by multiple factors associated with tissue development, such as microstructural proliferation and myelination.[59] The myelin volume which increases within the cortex across

development is a likely source of T1 changes. While the T1 in both white and grey matter is attributable primarily to myelin, it is also influenced by water content,[30,60] iron concentration[61,62] and macromolecular composition.[28] Future studies are necessary to examine the contributions to T1 abnormality of brain tissues in MDD.

Importantly, we found a negative correlation between T1 and GMV values of the left thalamus in MDD patients, which provides critical information for microstructural basis of macrostructural deficits in depression. Given the T1 is associated with multiple tissue characteristics,[28] the observed negative correlation between T1 and GMV indicates that the macrostructural morphologic alterations are related to macromolecular composition and local microenvironment of the left thalamus in MDD patients. Previous findings have shown development could create new tissue that displaces water, resulting in higher MTV and FA.[59] However, we did not observe any correlation between MTV and FA of the left thalamus, suggesting the microstructural alternations of the left thalamus may result from other biological factors such as axon diameter, axon density and myelin-sheath thickness.[63] Collectively, the microstructural properties of the thalamus are closely associated with its macroscopically structural abnormalities in MDD, providing microstructural evidence for structural abnormalities in depression.

Several limitations of the present study should be noted. As we did not collect the information of medication use, we cannot make strong inferences about how macroscopic and microstructural alternations of the thalamus might be affected by medication use. Future studies are necessary to replicate the findings across the first-episode, unmedicated patients. In addition, although our results were largely unchanged after controlling for participants' demographic variables, the MDD group and HCs were not matched for years of education. Despite that the methodology used in our study was relatively consistent and reliable, the combination of these methods in multi-modal MRI data analysis would weaken test-retest reliability due to the inherent limitations of specific methods. For example, probabilistic tractography can lead to unrealistic fibre tracts without anatomic justification, whereas morphometry measurements may be affected by analysis parameters. Although we used reliable methods for multi-modal analyses, corrected for multiple comparisons and controlled for covariate, the relatively small sample of the current study could also result in false positives of large effect sizes. Our findings need to be replicated with larger samples in future studies. Another limitation may come from the atlas we used in brain parcellation. Previous studies have shown unique advantage of specific parcellation/atlas for different modalities.[64,65] In line with previous studies, to make the optimal measure of each modality, we used Freesurfer built-in atlas and AAL atlas for subcortical volume measures and tractography analyses, respectively. Because the node definition by different parcellations could produce different connectivity patterns of brain networks,[66] the atlas used in the present study may have specific effects on the alternation of structural connectivity in MDD. Future studies can validate the consistency of structural connectivity across different parcellation schemes. The current study only focused on the microstructural alternations in specific regions associated with cross-modal macroscopic abnormalities, which restricted the exploration for whole-brain-wise microstructural features in MDD. Future studies can quantify qMRI measures across the whole brain and explore how microstructural properties altered in depression. Finally, the sample size of MDD patients and HCs were different in the current study, however, both MDD and HC samples were approximately normal distributed with the same variance. Therefore, the *t*-test we used in statistical analyses is applicable and reliable for group comparisons of different sample sizes.[67]

Conclusion

By using multi-modal neuroimaging techniques, we show consistently structural brain abnormalities in depression, from network connectivity, morphometric volume and thickness, to cytoarchitectonic-related properties. The LCSPT circuit plays a centric role in the structural brain alterations of depression, of which the thalamus is indispensable, with microstructural deficits underlying the macroscopic morphological changes. Our study sheds lights on the understanding of neuropathology of MDD and has important implications in the diagnosis and treatment of depression.

Acknowledgement

The authors declare that this work has been posted on medRxiv as a preprint (https://doi.org/10.1101/2021.10.11.21264842).

Funding

This work was supported by the National Natural Science Foundation of China (grants 31871137 and 31920103009), the Major Project of National Social Science Foundation (grants 20&ZD153), Young Elite Scientists Sponsorship Program by China Association for Science and Technology (grants YESS20180158), Guangdong International Scientific Collaboration Project (grants 2019A050510048), Natural Science Foundation of Guangdong Province (2020A1515011394), Shenzhen-Hong Kong Institute of Brain Science-Shenzhen Fundamental Research Institutions (grants 2019SHIBS0003), Shenzhen Science and Technology Research Funding Program (grants JCYJ2018 0507183500566, JCYJ20180306173253533 and JCYJ20190808121415365), Shenzhen Fund for Guangdong Provincial High-level Clinical Key Specialties (grants No. SZGSP013) and Shenzhen Key Medical Discipline Construction Fund (grants No.SZXK041).

Competing interests

The authors report no biomedical financial interests or potential conflicts of interest.

Supplementary material

Supplementary material is available at *Brain Communications* online.

Reference

1. Gotlib IH, Joormann J. Cognition and depression: Current status and future directions. *Annu Rev Clin Psychol*. 2010;6(1):285-312.
2. Drevets WC, Videen TO, Price JL, Preskorn SH, Carmichael ST, Raichle ME. A functional anatomical study of unipolar depression. *J Neurosci*. 1992;12(9):3628-3641.
3. Price JL, Drevets WC. Neurocircuitry of mood disorders. *Neuropsychopharmacology* 2010;35(1):192-216.
4. Swerdlow NR, Koob GF. Dopamine, schizophrenia, mania, and depression: Toward a unified hypothesis of cortico-striatopallido-thalamic function. *Behav Brain Sci*. 1987;10(2):197-208.
5. Sheline YI. Neuroimaging studies of mood disorder effects on the brain. *Biol Psychiatry* 2003;54(3):338-352.
6. Mayberg HS. Frontal lobe dysfunction in secondary depression. *J Neuropsychiatry Clin Neurosci*. 1994;6(4):428-442.
7. Drevets WC. Neuroimaging studies of mood disorders. *Biol Psychiatry* 2000;48(8):813-829.
8. Nugent AC, Davis RM, Zarate CA Jr, Drevets WC. Reduced thalamic volumes in major depressive disorder. *Psychiatry Res Neuroimaging* 2013;213(3):179-185.
9. Lu Y, Liang H, Han D, *et al.* The volumetric and shape changes of the putamen and thalamus in first episode, untreated major depressive disorder. *NeuroImage Clin*. 2016;11:658-666.
10. Koolschijn PCMP, van Haren NEM, Lensvelt-Mulders GJLM, Hulshoff Pol HE, Kahn RS. Brain volume abnormalities in major depressive disorder: A meta-analysis of magnetic resonance imaging studies. *Hum Brain Mapp*. 2009;30(11):3719-3735.
11. Krishnan KRR, McDonald WM, Escalona PR, *et al.* Magnetic resonance imaging of the caudate nuclei in depression: Preliminary observations. *Arch Gen Psychiatry* 1992;49(7):553-557.
12. Husain MM, McDonald WM, Doraiswamy PM, *et al.* A magnetic resonance imaging study of putamen nuclei in major depression. *Psychiatry Res Neuroimaging*. 1991;40(2):95-99.
13. Baumann B, Danos P, Krell D, *et al.* Reduced volume of limbic system–affiliated basal ganglia in mood disorders: Preliminary data from a postmortem study. *J Neuropsychiatry Clin Neurosci*. 1999;11(1):71-78.
14. Grieve SM, Korgaonkar MS, Koslow SH, Gordon E, Williams LM. Widespread reductions in gray matter volume in depression. *NeuroImage Clin*. 2013;3:332-339.
15. Schmaal L, Hibar DP, Sämann PG, *et al.* Cortical abnormalities in adults and adolescents with major depression based on brain scans from 20 cohorts worldwide in the ENIGMA Major Depressive Disorder Working Group. *Mol Psychiatry* 2017;22(6):900-909.
16. Bai F, Shu N, Yuan Y, *et al.* Topologically convergent and divergent structural connectivity patterns between patients with remitted geriatric depression and amnestic mild cognitive impairment. *J Neurosci*. 2012;32(12):4307-4318.
17. Long Z, Duan X, Wang Y, *et al.* Disrupted structural connectivity network in treatment-naive depression. *Prog Neuropsychopharmacology Biol Psychiatry* 2015;56:18-26.
18. Myung W, Han CE, Fava M, *et al.* Reduced frontal-subcortical white matter connectivity in association with suicidal ideation in major depressive disorder. *Transl Psychiatry* 2016;6(6):e835-e835.
19. Wang T, Wang K, Qu H, *et al.* Disorganized cortical thickness covariance network in major depressive disorder implicated by aberrant hubs in large-scale networks. *Sci Rep*. 2016;6(1):27964.
20. Xiong G, Dong D, Cheng C, *et al.* Potential structural trait markers of depression in the form of alterations in the structures of subcortical nuclei and structural covariance network properties. *NeuroImage Clin*. 2021;32:102871.
21. Haber S, Mcfarland NR. The place of the thalamus in frontal cortical-basal ganglia circuits. *Neuroscientist* 2001;7(4):315-324.
22. Keun JTB, van Heese EM, Laansma MA, *et al.* Structural assessment of thalamus morphology in brain disorders: A review and recommendation of thalamic nucleus segmentation and shape analysis. *Neurosci Biobehav Rev*. 2021;131:466-478.
23. Webb CA, Weber M, Mundy EA, Killgore WDS. Reduced gray matter volume in the anterior cingulate, orbitofrontal cortex and thalamus as a function of mild depressive symptoms: A voxel-based morphometric analysis. *Psychol Med*. 2014;44(13):2833-2843.
24. Korgaonkar MS, Fornito A, Williams LM, Grieve SM. Abnormal structural networks characterize major depressive disorder: A connectome analysis. *Biol Psychiatry*. 2014;76(7):567-574.
25. Jia Z, Wang Y, Huang X, *et al.* Impaired frontothalamic circuitry in suicidal patients with depression revealed by diffusion tensor imaging at 3.0 T. *J Psychiatry Neurosci*. 2014;39(3):170-177.
26. Singh MK, Kesler SR, Hosseini SM, *et al.* Anomalous gray matter structural networks in major depressive disorder. *Biol Psychiatry* 2013;74(10):777-785.
27. Ajilore O, Lamar M, Leow A, Zhang A, Yang S, Kumar A. Graph theory analysis of cortical-subcortical networks in late-life depression. *Am J Geriatr Psychiatry* 2014;22(2):195-206.
28. Mezer A, Yeatman JD, Stikov N, *et al.* Quantifying the local tissue volume and composition in individual brains with magnetic resonance imaging. *Nat Med*. 2013;19(12):1667-1672.
29. Weiskopf N, Mohammadi S, Lutti A, Callaghan MF. Advances in MRI-based computational neuroanatomy: From morphometry to in-vivo histology. *Curr Opin Neurol*. 2015;28(4):313-322.
30. Pomares FB, Funck T, Feier NA, *et al.* Histological underpinnings of grey matter changes in fibromyalgia investigated using multimodal brain imaging. *J Neurosci*. 2017;37(5):1090-1101.
31. Weiskopf N, Edwards LJ, Helms G, Mohammadi S, Kirilina E. Quantitative magnetic resonance imaging of brain anatomy and in vivo histology. *Nat Rev Phys*. 2021;3(8):570-588.
32. Gomez J, Barnett MA, Natu V, *et al.* Microstructural proliferation in human cortex is coupled with the development of face processing. *Science* 2017;355(6320):68-71.
33. Lerma-Usabiaga G, Carreiras M, Paz-Alonso PM. Converging evidence for functional and structural segregation within the left ventral occipitotemporal cortex in reading. *Proc Natl Acad Sci U S A*. 2018;115(42):E9981-E9990.
34. Oishi H, Takemura H, Aoki SC, Fujita I, Amano K. Microstructural properties of the vertical occipital fasciculus explain the variability in human stereoacuity. *Proc Natl Acad Sci U S A*. 2018;115(48):12289-12294.
35. Natu VS, Gomez J, Barnett M, *et al.* Apparent thinning of human visual cortex during childhood is associated with myelination. *Proc Natl Acad Sci U S A*. 2019;116(41):20750-20759.
36. Sacchet MD, Gotlib IH. Myelination of the brain in major depressive disorder: An in vivo quantitative magnetic resonance imaging study. *Sci Rep*. 2017;7(1):2200.
37. Kitzbichler MG, Aruldass AR, Barker GJ, *et al.* Peripheral inflammation is associated with micro-structural and functional connectivity changes in depression-related brain networks. *Mol Psychiatry* 2021;26(12):7346-7354.

38. Zalesky A, Fornito A, Bullmore ET. Network-based statistic: Identifying differences in brain networks. *Neuroimage* 2010; 53(4):1197-1207.
39. Tzourio-Mazoyer N, Landeau B, Papathanassiou D, *et al.* Automated anatomical labeling of activations in SPM using a macroscopic anatomical parcellation of the MNI MRI single-subject brain. *Neuroimage* 2002;15(1):273-289.
40. Schaefer A, Kong R, Gordon EM, *et al.* Local-global parcellation of the human cerebral cortex from intrinsic functional connectivity MRI. *Cereb Cortex* 2018;28(9):3095-3114.
41. Fischl B, Salat DH, Busa E, *et al.* Whole brain segmentation: Automated labeling of neuroanatomical structures in the human brain. *Neuron* 2002;33(3):341-355.
42. Fischl B, Van Der Kouwe A, Destrieux C, *et al.* Automatically parcellating the human cerebral cortex. *Cereb Cortex* 2004;14(1): 11-22.
43. Phillips ML, Drevets WC, Rauch SL, Lane R. Neurobiology of emotion perception I: The neural basis of normal emotion perception. *Biol Psychiatry* 2003;54(5):504-514.
44. Drevets WC, Price JL, Furey ML. Brain structural and functional abnormalities in mood disorders: Implications for neurocircuitry models of depression. *Brain Struct Funct*. 2008; 213(1-2):93-118.
45. Anticevic A, Cole MW, Repovs G, *et al.* Characterizing thalamocortical disturbances in schizophrenia and bipolar illness. *Cereb Cortex* 2014;24(12):3116-3130.
46. Anticevic A, Cole MW, Murray JD, Corlett PR, Wang XJ, Krystal JH. The role of default network deactivation in cognition and disease. *Trends Cogn Sci*. 2012;16(12):584-592.
47. Uddin LQ. Salience processing and insular cortical function and dysfunction. *Nat Rev Neurosci*. 2015;16(1):55-61.
48. Menon V. Large-scale brain networks and psychopathology: A unifying triple network model. *Trends Cogn Sci*. 2011;15(10): 483-506.
49. Gong Q, He Y. Depression, neuroimaging and connectomics: A selective overview. *Biol Psychiatry* 2015;77(3):223-235.
50. Bora E, Harrison BJ, Davey CG, Yücel M, Pantelis C. Meta-analysis of volumetric abnormalities in cortico-striatal-pallidal-thalamic circuits in major depressive disorder. *Psychol Med*. 2012;42(4): 671-681.
51. Wagner G, Koch K, Schachtzabel C, Schultz CC, Sauer H, Schlösser RG. Structural brain alterations in patients with major depressive disorder and high risk for suicide: Evidence for a distinct neurobiological entity? *Neuroimage* 2011;54(2):1607-1614.
52. Bremner JD, Narayan M, Anderson ER, Staib LH, Miller HL, Charney DS. Hippocampal volume reduction in major depression. *Am J Psychiatry* 2000;157(1):115-118.
53. Bora E, Fornito A, Pantelis C, Yücel M. Gray matter abnormalities in major depressive disorder: A meta-analysis of voxel based morphometry studies. *J Affect Disord*. 2012;138(1-2):9-18.
54. Suh JS, Schneider MA, Minuzzi L, *et al.* Cortical thickness in major depressive disorder: A systematic review and meta-analysis. *Prog Neuropsychopharmacol Biol Psychiatry* 2019;88: 287-302.
55. Price JL, Drevets WC. Neural circuits underlying the pathophysiology of mood disorders. *Trends Cogn Sci*. 2012;16(1):61-71.
56. Disner SG, Beevers CG, Haigh EAP, Beck AT. Neural mechanisms of the cognitive model of depression. *Nat Rev Neurosci*. 2011; 12(8):467-477.
57. Fales CL, Barch DM, Rundle MM, *et al.* Altered emotional interference processing in affective and cognitive-control brain circuitry in major depression. *Biol Psychiatry*. 2008;63(4):377-384.
58. Anand A, Li Y, Wang Y, *et al.* Activity and connectivity of brain mood regulating circuit in depression: A functional magnetic resonance study. *Biol Psychiatry* 2005;57(10):1079-1088.
59. Yeatman JD, Wandell BA, Mezer AA. Lifespan maturation and degeneration of human brain white matter. *Nat Commun*. 2014;5(1):4932.
60. Filo S, Shtangel O, Salamon N, *et al.* Disentangling molecular alterations from water-content changes in the aging human brain using quantitative MRI. *Nat Commun*. 2019;10(1):3403.
61. Stüber C, Morawski M, Schäfer A, *et al.* Myelin and iron concentration in the human brain: A quantitative study of MRI contrast. *Neuroimage* 2014;93:95-106.
62. Möller HE, Bossoni L, Connor JR, *et al.* Iron, myelin, and the brain: Neuroimaging meets neurobiology. *Trends Neurosci*. 2019;42(6): 384-401.
63. Basser PJ, Pierpaoli C. Microstructural and physiological features of tissues elucidated by quantitative-diffusion-tensor MRI. *J Magn Reson*. 2011;213(2):560-570.
64. Lerch JP, Van Der Kouwe AJW, Raznahan A, *et al.* Studying neuroanatomy using MRI. *Nat Neurosci*. 2017;20(3):314-326.
65. Raj A, Kuceyeski A, Weiner M. A network diffusion model of disease progression in dementia. *Neuron* 2012;73(6):1204-1215.
66. Zalesky A, Fornito A, Harding IH, *et al.* Whole-brain anatomical networks: Does the choice of nodes matter? *Neuroimage* 2010; 50(3):970-983.
67. Armitage P, Berry G, Matthews JNS. *Statistical Methods in Medical Research*. John Wiley & Sons; 2008.